beverages

Article

Ethanol's Pharmacodynamic Effect on Odorant Detection in Distilled Spirits Models

Zhuzhu Wang [1] and Keith R. Cadwallader [2,*]

[1] Archer-Daniels-Midland Company (ADM), 1001 N Brush College Road, Decatur, IL 62521, USA; zhuzhu.wang@adm.com
[2] Department of Food Science and Human Nutrition, University of Illinois, 1302 W. Pennsylvania Ave., Urbana, IL 61801, USA
* Correspondence: cadwlldr@illinois.edu

Abstract: Aroma perception in distilled spirits is influenced by both the physicochemical and pharmacodynamic effects of ethanol. This study measured these effects by examining the odor detection threshold (ODT) of various odorants. The physicochemical effect influences how odorants partition into the vapor matrix (headspace), while the pharmacodynamic effect affects the functioning of olfactory receptors cells (ORCs). Both factors contribute to changes in odorant ODTs, though it remains unclear which has a greater influence. Across three exploratory experiments, we demonstrated that ethanol in the vapor matrix suppressed the olfactory detection of key odorants in distilled spirits, with some chemical groups being more affected than others. This suppression effect increased as ethanol concentration rose. Notably, our results showed that ethanol's pharmacodynamic effect plays the primary role in elevating ODTs in ethanol/water solutions, and this effect intensifies as ethanol concentration in the liquid matrix increases. These findings highlight the significant role of ethanol concentration in the vapor matrix and provide scientific support for practices such as diluting spirits or using specifically shaped glassware to lower ethanol headspace concentration during whiskey nosing (odor evaluation).

Keywords: ethanol; distilled spirits; odorant perception; pharmacodynamic

Citation: Wang, Z.; Cadwallader, K.R. Ethanol's Pharmacodynamic Effect on Odorant Detection in Distilled Spirits Models. *Beverages* **2024**, *10*, 116. https://doi.org/10.3390/beverages10040116

Academic Editor: Enrique Durán-Guerrero

Received: 25 October 2024
Revised: 20 November 2024
Accepted: 22 November 2024
Published: 26 November 2024

1. Introduction

Beyond pricing, consumers in the global spirits market are primarily drawn to various brands based on the sensory attributes, including aroma, taste, and mouthfeel. Consequently, enhancing the organoleptic quality of distilled spirits has long been a strategic goal for the alcoholic beverage industry. While significant research has focused on the odor- and taste-active components of distilled spirits [1–4], there is, however, a notable gap in the published work regarding the effect of ethanol—one of the most organoleptically influential components across all distilled spirits—on sensory perception.

Ethanol plays a significantly role in shaping the perceived aroma profile of alcoholic beverages such as wine, beer, and distilled spirit [5–8]. Its concentration affects the solubility of odorants in solution, influencing how these compounds partition into the vapor matrix [6,9]. This effect, often referred to as ethanol's physicochemical effect, has led to the widely recognized practice of diluting ethanol content (e.g., from 40% ABV to 20% ABV) to enhance aroma perception during nosing. Dilution is believed to promote the release of more volatile compounds into the headspace, enriching the overall perceived flavor profile [5–9]. However, what has been overlooked is that dilution of ethanol in the solution also leads to significant reduction in its concentration in the headspace. Given the published findings on ethanol's pharmacodynamic effects—which include decreasing olfactory sensitivity [10,11], depressing synaptic excitation in the olfactory bulb and synaptic transmission in the olfactory cortex [12,13], and altering lipid bilayer membrane properties and modulating membrane protein functions [14–17], a mechanism similar to sensory masking [18] and "off-target" drug

effect [19]—it is reasonable to conclude that reducing ethanol concentration in the headspace may influence its interaction with olfactory receptor cells (ORCs). This effect likely contributes to the observed shift in the overall perceived flavor profile. To the best of our knowledge, no studies have directly addressed how ethanol's pharmacodynamic effect alone impacts the perception of flavor profiles in distilled spirits [5]. In a flavor profile, the ODT of individual odorants plays an essential role, as it influences the detectability of each odorant and, consequently, contributes to overall flavor perception. While variations in the ODT of odorants in ethanol/water solutions have been documented [5]—likely influenced by ethanol's physicochemical effect on odorant partitioning in the headspace—our group is the first to report that ethanol's pharmacodynamic effect independently affects odorant detection by altering ethanol concentration in the vapor matrix [5].

In this study, our primary objective is to further evaluate the impact of ethanol's pharmacodynamic effect on odorant detection in distilled spirits models, extending our analysis across a diverse range of chemical groups—including esters, aldehydes, ketones, alcohols, acids, lactones, phenols, and hydrocarbons—to ensure that our findings are comprehensive and representative of the various chemical categories contributing to flavor profile of distilled spirits. Our second objective is to test our hypothesis that changes in odorant ODTs are primarily driven by ethanol's pharmacodynamic effects, resulting from variations in ethanol concentration in the liquid matrix, which subsequently alters ethanol concentration in the vapor matrix. To address these objectives, we carefully designed and executed three experiments, allowing us to demonstrate how ethanol's pharmacodynamic effect impact the ODT of key odorants in distilled spirits models and to identify the dominant ethanol-related factors influencing odorant detection in ethanol/water solutions.

2. Materials and Methods

2.1. Chemicals

Ethanol (CAS No. 64-17-5, 200 proof, Decon Labs, Inc. (King of Prussia, PA, USA), ethyl isobutyrate (CAS No. 97-62-1), ethyl isovalerate (CAS No. 108-64-5), 3-methyl-1-butanol (CAS No. 123-51-3), linalool (*R*/*S*) (CAS No. 78-70-6), isovaleric acid (CAS No. 503-74-2), whiskey lactone (*E* and *Z*) (CAS No. 39212-23-2), octanoic acid (CAS No. 124-07-2), syringol (CAS No. 91-10-1), ethyl propionate (CAS No. 105-37-3), ethyl butyrate (CAS No. 105-54-4), isoamyl acetate (CAS No. 123-92-2), 2-octenal (CAS No. 2548-87-0), butyric acid (CAS No. 107-92-6), β-damascenone (CAS No. 23696-86-7, 1.1–1.4 wt.% in 190 proof ethanol, used in the first experiment), 2-phenylethanol (CAS No. 60-12-8), γ-decalactone (CAS No. 706-14-9), isoeugenol (*E*) (CAS No. 97-54-1), p-cymene (CAS No. 99-87-6), ethyl octanoate (CAS No. 106-32-1), α-terpineol (CAS No. 98-55-5), guaiacol (CAS No. 90-05-1), β-ionone (CAS No. 14901-07-6), vanillin (CAS No. 121-33-5), β-myrcene (CAS No. 123-35-3), γ-terpinene (CAS No. 99-85-4), *cis*-3-hexen-1-ol (CAS No. 928-96-1), ethyl decanoate (CAS No. 110-38-3), phenethyl acetate (CAS No. 103-45-7), 4-ethylguaiacol (CAS No. 2785-89-9) and eugenol (CAS No. 97-53-0) were purchased from Sigma-Aldrich (St. Louis, MO, USA). β-damascenone (used in the second experiment) was obtained from Firmenich (Geneva, Swetzerland), p-cresol (CAS No. 106-44-5), γ-nonalactone (CAS No. 104-61-0), 4-ethylphenol (CAS No. 123-07-9) were obtained from Aldrich F&F. Chemical purities were determined using a 6890 GC (Agilent Technologies, Inc., Palo Alto, CA, USA) equipped with a flame ionization detector (FID) and HP-5 column (30 m length × 0.32 mm i.d. × 0.25 μm film thickness; Agilent, Palo Alto, CA, USA). All odorants were determined to be free of any odor impurities by analysis of 100-ppm solution by gas chromatography olfactometry (GC-O, method discussed later), and any odorants that were found to be odor impure were further purified through flash (silica gel) chromatography.

2.2. Evaluate Ethanol's Pharmacodynamic Effect Alone on ODT of Key Odorants in Distilled Spirits Models

In this experiment, we eliminated the presence of the "spirits liquid matrix" (ethanol/water solutions with varying alcohol-by-volume (ABV) values) and evaluated changes in ODTs of odorants as ethanol concentrations increased in the vapor matrix.

GC-O can be modified and developed to study odor mixtures [20]. By introducing a background odor into the olfactometry air and mixing it with the GC effluent, it is possible to evaluate the detection of one odorant in the presence of another constant odor background. This method, originally published by Wang et al. [6], was applied here with modifications—the constant "odor background" is a vapor matrix equivalent to the dynamic headspace above pure water, 20%, and 40% ABV ethanol/water solutions (denoted as 0% $ABV_{d.equiv.}$, 20% $ABV_{d.equiv.}$, 40% $ABV_{d.equiv.}$, respectively). We then calculated the degree of ODT change (R) as ethanol concentration in the vapor matrix increased from 0% $ABV_{d.equiv.}$ to 20% $ABV_{d.equiv.}$ and 40% $ABV_{d.equiv.}$ and identified which chemical group(s) were more affected than others.

The first step was to determine the corresponding ethanol concentration at 20% $ABV_{d.equiv.}$, or 40% $ABV_{d.equiv.}$. To do so, a standard curve was firstly established using the total vaporization technique (TVT). Ethanol was added in varying amounts (0.5, 1, 2, 6, 10, 30, and 60 µL) to a consistent volume (60 mL) of headspace vials equipped with PTFE-lined silicone septa. After equilibrating at room temperature for at least 2 h, a 50 µL sample of headspace was withdrawn using a 100-µL gas-tight syringe preheated to 30 °C. The Samples were injected hot split 6:1 into a 6890 GC (Agilent Technologies, Inc., Palo Alto, CA, USA) equipped with a FID and RTX-Wax® column (10 m length × 0.53 mm i.d. × 1 µm film thickness; Restek Corp., Bellefonte, PA, USA). Helium was used as the carrier gas at a constant flow rate of 5.0 mL/min. The GC inlet temperature was set at 250 °C, and the oven was maintained at 40 °C throughout the 5-min run. Ethanol peak areas were plotted against the ethanol concentration in the vials. It was observed that when 30 and 60 µL of ethanol were introduced, a condensed phase formed in the vials, indicating that ethanol concentration in the vapor phase had exceeded that of saturated vapor, causing the standard curve to flatten at these higher ethanol concentrations. Therefore, only the first five ethanol concentrations were used for the standard curve, as their correlation with ethanol peak area was linear. Secondly, a NEAT brand spirits glass was filled with 44 mL of ethanol/water solution at 20% ABV and 40% ABV, respectively, and placed in a water bath maintained at 26 °C. The water level was kept at the height of the glass edge. After reaching equilibrium, 50 µL of dynamic headspace vapor was sampled using a preheated (30 °C) gas-tight syringe positioned at the center of rim. The sample was immediately injected into the GC using the previously described parameters. Ethanol peak areas were recorded, and concentrations were calculated based on the standard curve. The ethanol concentration for the 20% $ABV_{d.equiv.}$ was found to be 9.9 ± 1.3 mg/L in air, and for the 40% $ABV_{d.equiv.}$, it was 17.01 ± 0.61 mg/L in air.

The second step was to establish the 0% $ABV_{d.equiv.}$, 20% $ABV_{d.equiv.}$, or 40% $ABV_{d.equiv.}$ vapor matrices. To do so, 500 mL of odorless water and 500 mL of ethanol were placed in separate 1 L glass bottles fitted with two-port caps. An odorless, dry air flow (15–17 L/min) was split into two streams, with each stream directed onto the surface of the liquid in the bottles through one port. Both bottles were placed in a water bath maintained at 30 °C to prevent evaporative cooling. The saturated vapor streams from the two bottles were then combined and directed to the odor detection port (ODP, Datu Technologies, Geneva, NY, USA). Two flow meters (Cole-Parmer, Vernon Hills, IL, USA) positioned between the air source and the bottles were used to control the flow rate of the two streams. Once equilibrium was reached, 50 µL of the vapor matrix at the end of ODP was sampled using a preheated (30 °C) gas-tight syringe and analyzed by GC using the previously described method. Ethanol concentrations were calculated from the ethanol peak areas based on the standard curve. This process was repeated until the ethanol concentration reached 9.9 ± 1.3 mg/L for 20% $ABV_{d.equiv.}$, and 17.01 ± 0.61 mg/L for 40% $ABV_{d.equiv.}$. This GC-O set up was capable of

delivering a defined and stable concentration of air-water-ethanol vapor matrix for at least 1 h (Figure 1).

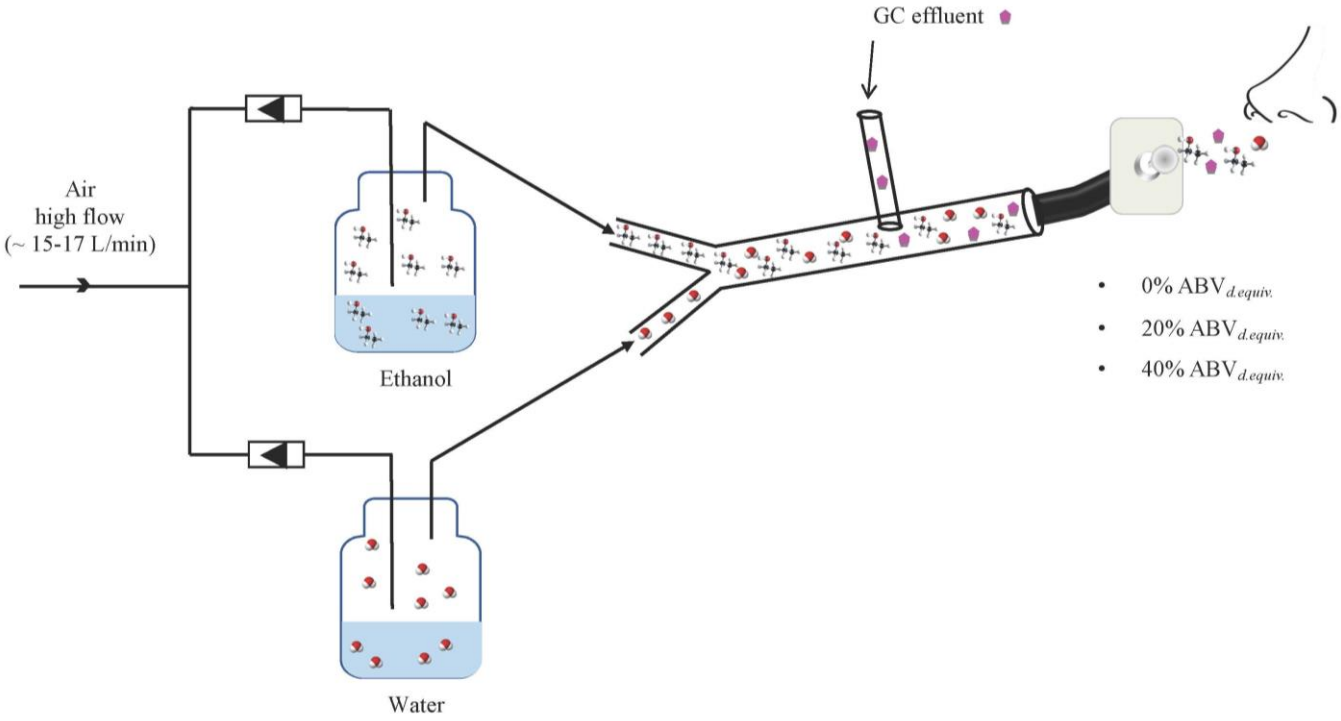

Figure 1. Schematic of GC-O set up for the determination of the GCO of odorants in 0% $ABV_{d.equiv.}$, 20% $ABV_{d.equiv.}$, and 40% $ABV_{d.equiv.}$ vapor matrices.

Three panelists (panel 1, consisting of 3 females aged 21–35 yrs) were selected for this experiment based on their ability to detect forty-six odorants on GC-O in a 0% $ABV_{d.equiv.}$ vapor matrix at the expected retention times and to provide proper description of the odor qualities. All participants gave informed consent prior to conducting the experiment with the approval of the Institutional Review Board (IRB) at the University of Illinois Urbana-Champaign (IRB Protocol Number: 17508). Among the forty-six odorants, three were classified as "generalists", twenty-two as "intermediaries", and six as "individualists" key food odorants (KFO) across 227 food samples spinning a wide range of categories [21]. The remaining fifteen odorants were chosen based on published literature where they were identified as important odorant in distilled spirits.

All forty-six odorants were randomly divided into three groups and dissolved in diethyl ether at a concentration of approximately 20 ppm. Participants were given brief introduction to GC-O and instructed to position their nose near the ODP, record the retention time when an odor was detected, and provide a description of the odor quality. Participants were unaware of the total number of odorants but were informed that each group's evaluation would conclude after 30 min. The GC-O system consisted of a 6890 GC (Agilent Technologies, Inc., Palo Alto, CA, USA) equipped with a cool on-column injector and ODP. Each group (2 µL) was injected and separated using an RTX®-Wax column (15 m length × 0.53 mm i.d. × 1.0 µm film thickness; Resteck Corp., Bellefonte, PA, USA). Helium was used as the carrier gas at a constant flow rate of 5.0 mL/min. The oven temperature program was as follows: initial temperature of 35 °C with a 5-min hold, followed by a ramp of 10 °C/min to a final temperature of 225 °C, which was held for 30 min.

In this experiment, thirty-four odorants from the original list of forty-six were then selected and strategically divided into four groups based on their relative GC-O elution order, ensuring that the time gap between each odorant was greater than two minutes. This gap allowed sufficient time for panelists to recover from exposure to the odorant and ethanol, alleviating olfactory fatigue. Additionally, strict protocols were implemented. Panelists were

instructed to begin sniffing (engaging with the ODP) 15 s prior to the expected retention time (elution time) of each odorant and to stay engaged until 15 s after the elution of the odorant. After that, panelists sniffed their sleeves and breathed clean, odor-free air to help their olfactory senses return to a normal state before sniffing the next odorant.

Each stock solution of these four group odorants was prepared in diethyl ether and then stepwise diluted 1:3 (*v*/*v*) in the same solvent. Panelists evaluated each dilution from the low concentration (highest dilution) and proceeded toward higher concentration in 0% $ABV_{d.equiv.}$ vapor matrix, then evaluated each dilution again from the high concentration and proceeded toward lower concentration in other two vapor matrices (20% $ABV_{d.equiv.}$ and 40% $ABV_{d.equiv.}$) under the same GC-O conditions. If an odorant was not detected in the 1:3 dilution, then the undiluted stock solution was used. The evaluation concluded when no odorants were detectable in two consecutive dilutions. For each panelist, the ODT of each odorant was calculated as individual Best Estimate Threshold (BET), expressed in µg, which is the geometric mean of mass at which the last detection occurred and the next lower (adjacent) mass, following the guideline of ASTM E679-19 [22]. BETs are hereafter referred through the manuscript as ODTs.

2.3. Evaluate Changes in ODT of Key Odorants in Distilled Spirits Models as a Result of Both Ethanol's Physicochemical and Pharmacodynamic Effects

In this experiment, we included the "spirits liquid matrix" and evaluated changes in ODT as the ethanol concentration increased from 0% to 20%, and then to 40% in the ethanol/water solution. The same panel from this experiment also conducted the GC-O threshold test described earlier. We compared the degree of ODT change (R) for the same odorants between ethanol concentration changes in the liquid matrices versus the vapor matrices.

Seven odorants from the list of thirty-four were selected for this experiment, including 4-ethylguaiacol, ethyl isobutyrate, β-damascenone, ethyl butyrate, guaiacol, γ-nonalactone, and isoeugenol. Following the method described by Buttery et al. [23], a stock solution of each odorant—free of any odor impurities, confirmed by analysis of a 100-ppm solution via GC-O—was prepared by dissolving the odorant in 10 mL of ethanol, then a known volume of each stock solution was spiked into the first PTFE sniff bottle containing 30 mL of either water (0%), 20%, or 40% ABV ethanol/water solutions. A stepwise 1:3 (*v*/*v*) dilution was prepared by adding 20 mL of the corresponding ethanol/water solution to a new sniff bottle, followed by adding 10 mL of the previously spiked solution. The final volume in each sniff bottle was 20 mL.

The triangle test method was used during evaluation, where each diluted odorant was presented alongside two blanks (20 mL of water, 20%, or 40% ABV ethanol/waster solutions in the sniff bottles). A series of six ascending concentrations for each odorant in each ethanol/water solution were tested. A new panel (panel 2), consisting of two females and two males aged 21–35 yrs, was selected for this experiment. The panel 2 was familiar with these seven chosen odorants and has had extensive experience with GC-O. Panelists were instructed to sniff each sample within each set and identify the sample that differed from the other two. To prevent olfactory fatigue and adaptation from repeated exposure to ethanol, a timer was used between each sample evaluation, ensuring panelists took a break (~7 s) between each evaluation.

For each panelist, the ODT of each odorant was calculated as the individual BET, expressed in ppb, according to ASTM E679-19 [22]. Additionally, for each panelist in panel 2, individual ODTs of the seven odorants were determined in the 0% $ABV_{d.equiv.}$, 20% $ABV_{d.equiv.}$, and 40% $ABV_{d.equiv.}$ vapor matrices using the previously described method.

2.4. Evalaute the Physicochemical Effect of Ethanol on the Partioning of Odorants in the Vapor Matrix

In this experiment, we determined the gas/liquid partition coefficient (k_i) of key odorants in 0% ABV (water), 20% ABV, and 40% ABV ethanol/water solutions by equilibrium headspace-gas-chromatography (EHS-GC) utilizing the phase ratio variation method.

k_i is defined as the ratio of the concentration of an odorant in the gas phase to its concentration in the liquid phase. Using the method described by Ettre et al. [24], glass headspace vials (20 mL, Resteck) were filled with varying volumes (1, 2, 3, and 4 mL) of water, 20%, or 40% ABV ethanol/water solutions containing each of the seven odorants (4-ethylguaiacol, ethyl isobutyrate, β-damascenone, ethyl butyrate, guaiacol, γ-nonalactone, and isoeugenol). The vials were sealed with a PTFE-lined septa/metallic caps (Resteck), and EHS-GC analysis was performed using a CombiPal autosampler (Leap Technologies, Inc., Morrisville, NC, USA). After equilibrating at 30 °C (300 rpm) for 30 min, a 1 mL sample of the headspace was automatically withdrawn with a 2.5 mL gas-tight syringe (filling rate was 100 µL/s, 1 fill stroke) preheated to 45 °C. The sample was then injected in hot split mode (250 °C, 6:1) into the GC-MS system at an injection speed of 100 µL/s. The GC-MS system consisted of a 6890 N GC equipped with a RXI-5Sil MS column (30 m length × 250 µm i.d. × 0.25 µm film thickness; Resteck Corp., Bellefonte, PA, USA), and a 5973 N mass spectrometer (Agilent Technologies Inc.). Helium was used as the carrier gas at a constant flow rate of 1 mL/min. The oven temperature program was as follows: initial temperature of 30 °C with a 5-min hold, followed by a ramp of 10 °C/min to a final temperature of 200 °C, which was held for 15 min. Only one injection was made per vial, and duplicate vials were analyzed for each solution, with peak area values averaged from two separated injections. For each odorant in each ethanol/water solution, two replications were performed, and the k_i value reported here represent the mean of these replicates.

For β-damascenone and isoeugenol, the k_i values were determined at 60 °C using the same GC-MS system. After equilibrium at 60 °C for 30 min, a 1 mL headspace sample was automatically withdrawn with the same 2.5 mL gas-tight syringe preheated to 70 °C and injected in hot split mode into the GC-MS system.

For γ-nonalactone, the k_i value was determined at 60 °C using the same GC-MS system but equipped with a Stabilwax®-DA column (30 m length × 250 µm i.d. × 0.25 µm film thickness; Resteck Corp., Bellefonte, PA, USA). The injection was hot split (250 °C, 2.5:1), and the oven temperature program was as follows: initial temperature of 30 °C with a 5-min hold, followed by a ramp of 10 °C/min to a final temperature of 200 °C, which was held for 30 min. All other parameters were consistent with the conditions described earlier.

2.5. Statistical Analsyis

Shapiro-Wilk test was employed to check for normality. Kruskal-Wallis Test was performed to assess the differences among chemical groups. Nonparametric pair comparisons were performed using Wilcoxon method. The analyses were conducted using JMP® (version Pro 17. SAS Institute Inc., Cary, NC, USA, 1989–2023). Adjusted *p*-value analysis were performed using R statistical Software (v4.3.1; R Core Team 2023).

3. Results

3.1. ODTs of Odorants in the 0% $ABV_{d.equiv.}$, 20% $ABV_{d.equiv.}$, and 40% $ABV_{d.equiv.}$ Vapor Matrices (Experiment 1)

Table S1 lists the ODTs of all three panelists for the thirty-four tested odorants in the vapor matrices of 0% $ABV_{d.equiv.}$, 20% $ABV_{d.equiv.}$, or 40% $ABV_{d.equiv.}$. From an individual perspective, each panelist' ODT varies for each odorant across the different vapor matrices due to their varying sensitivity to odor detection and identification [25,26]. However, when considering the data holistically (Figure 2)—grouping the ODTs of all three panelists by chemical groups and differentiating them by vapor matrices—a clear trend emerges: as ethanol concentration increases in the vapor matrix, the ODT of all tested odorants rises. This effect is particularly pronounced for certain chemical groups, such as alcohols, esters, hydrocarbons, and phenols, indicating that the detection of these groups is more suppressed in vapor matrices of high ethanol concentration.

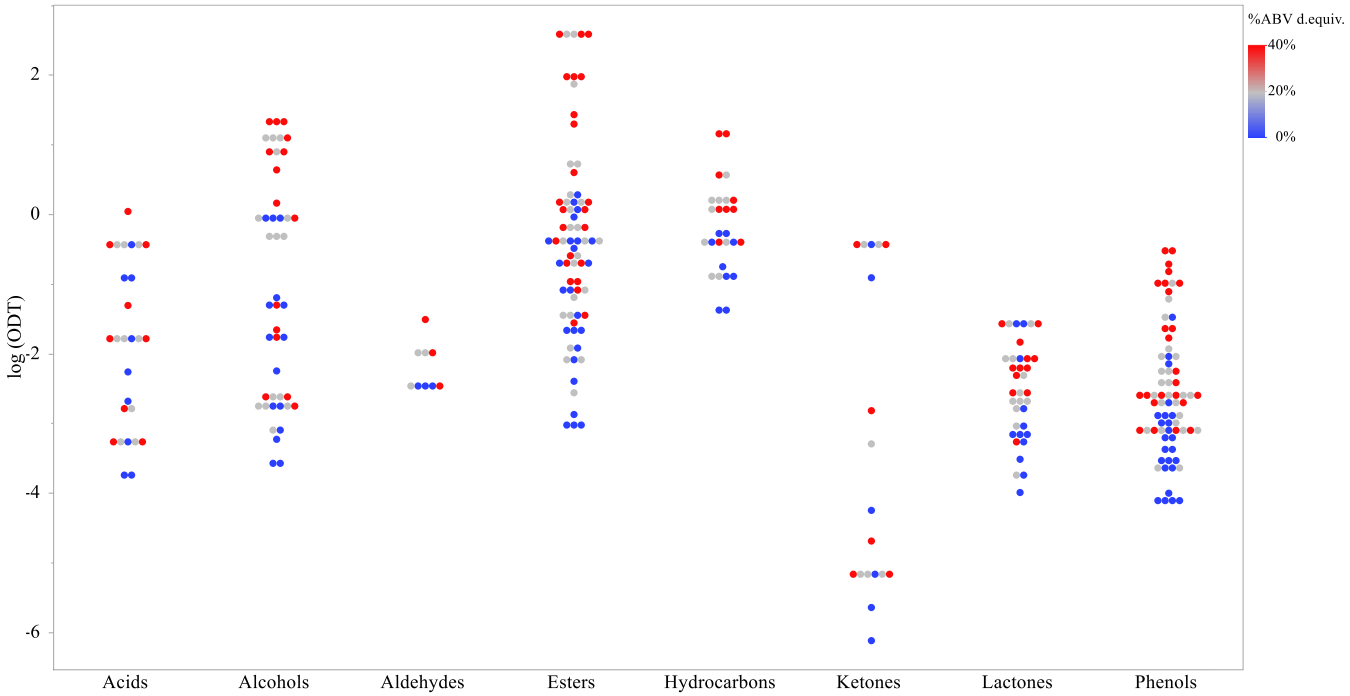

Figure 2. ODT results in log scale for each tested odorant, grouped by chemical group, in vapor matrices of 0% $ABV_{d.equiv.}$, 20% $ABV_{d.equiv.}$, and 40% $ABV_{d.equiv.}$.

Using an approach previously described in the literature [27], the degree of ODT change (R) is obtained as the ratio of individual ODT determined in the vapor matrices of either 20% $ABV_{d.equiv.}$ or 40% $ABV_{d.equiv.}$ versus that determined in 0% $ABV_{d.equiv.}$ (denoted as $R_{20\%ABV\ d.equiv.}$ and $R_{40\%ABV\ d.equiv.}$, respectively). In Figure 3, the $R_{20\%ABV\ d.equiv.}$ and $R_{40\%ABV\ d.equiv.}$ values for all three panelists, expressed in log scale, are plotted for each chemical group. At first glance, the data for each group does not appear to follow a normal distribution, with varying degree of skewness. This skewness suggests that, even within each chemical group, there are differences between individual chemicals—the detection of certain chemicals is more suppressed than others when ethanol is present in the vapor matrices. The Shapira-Wilk tests conducted on $R_{20\%ABV\ d.equiv.}$ and $R_{40\%ABV\ d.equiv.}$ values of esters confirmed the lack of normality (p = 0.00047, and p = 0.037, respectively), so the non-parametric tests, such as the Kruskal-Wallis Test, was utilized for all subsequent statistical analyses.

The Kruskal-Wallis Test showed that there were no significant differences in $R_{20\%ABV\ d.equiv.}$ between the various chemical groups, $\chi^2 = 7.32$, $p = 0.3968$. However, there were significant differences in $R_{40\%ABV\ d.equiv.}$ between the chemical groups, $\chi^2 = 18.05$, $p = 0.0118$. The initial post-hoc analysis with Wilcoxon method, before adjusting for multiple comparisons, indicated statistically significant differences between certain group pairs, with p-values below the conventional 0.05 threshold (Table 1). However, after applying the Benjamini-Hochberg (BH) correction to control for the false discovery rate, the adjusted p-values for these comparisons increased, and some of them no longer met the 0.05 significance threshold. Despite this, a few of the adjusted p-values remain below 0.1, indicating marginal significance between phenols and acids, and alcohols and acids.

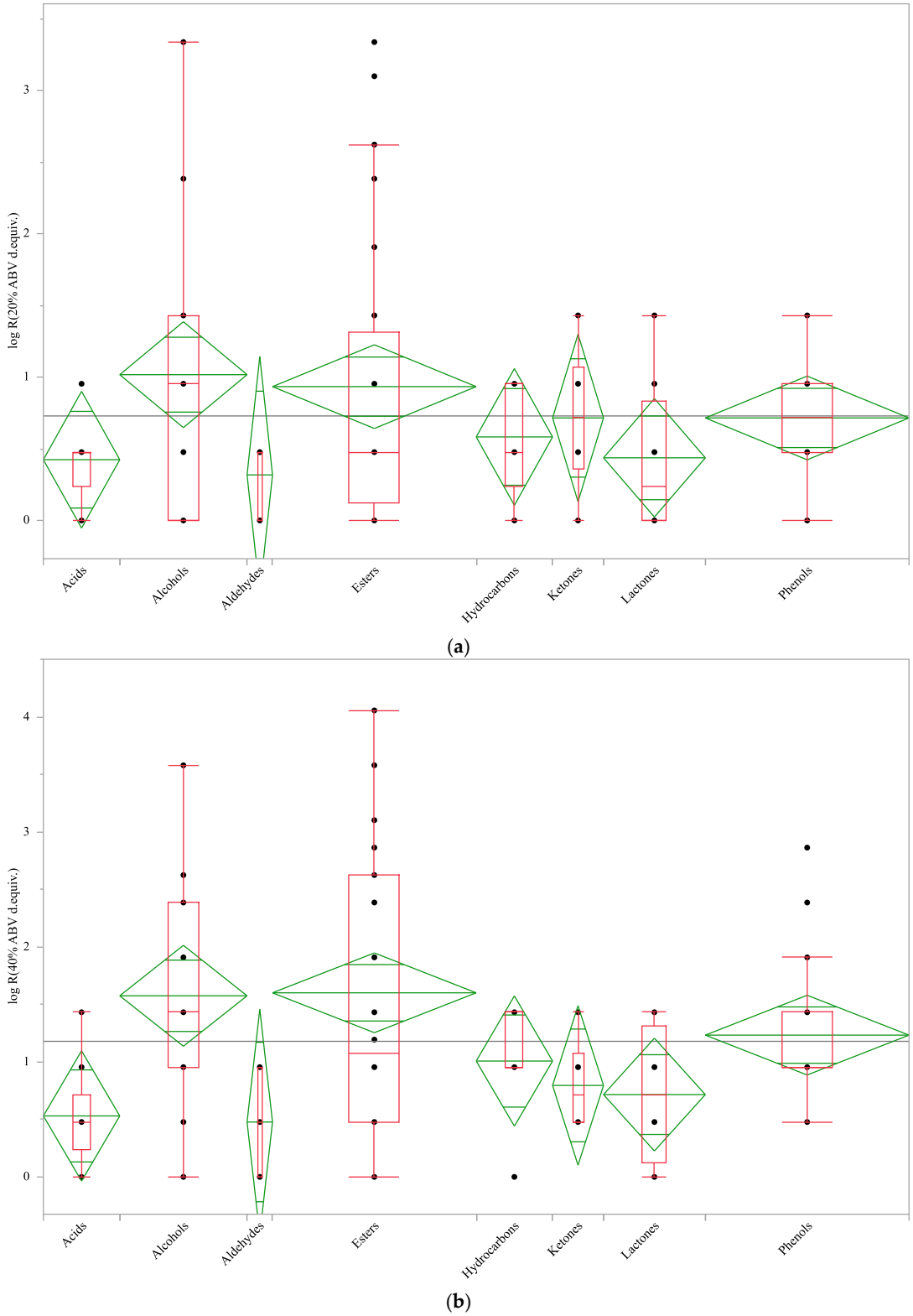

Figure 3. (**a**) Results for $R_{20\%ABV\ d.equiv.}$ expressed in log scale for each tested odorant, grouped by chemical group; (**b**) Results for $R_{40\%ABV\ d.equiv.}$ expressed in log scale for each tested odorant, grouped by chemical group.

Table 1. Post-hoc nonparametric comparison for each $R_{40\%ABV\ d.equiv.}$ pair on log scale using Wilcoxon method with Benjamini-Hochberg (BH) correction.

Comparison	Z Score	*p*-Value	Adjusted *p*-Value	Effect Size (r)
Phenols vs. Acids	2.879	0.0040 *	0.0728 **	0.51
Phenols vs. Aldehydes	1.878	0.0604 **	0.1868	0.36
Esters vs. Acids	2.318	0.0204 *	0.1547	0.40
Alcohols vs. Acids	2.792	0.0052 *	0.0728 **	0.57
Esters vs. Aldehydes	1.520	0.1285	0.2768	0.29
Phenols vs. Lactones	2.007	0.0448 *	0.1868	0.33
Phenols vs. Ketones	1.537	0.1243	0.2768	0.28
Hydrocarbons vs. Acids	2.107	0.0351 *	0.1868	0.50
Hydrocarbons vs. Aldehydes	1.595	0.1107	0.2768	0.46
Ketones vs. Acids	1.222	0.2217	0.3857	0.32
Lactones vs. Acids	0.7411	0.4586	0.5847	0.16
Lactones vs. Aldehydes	0.5957	0.5514	0.6663	0.15
Phenols vs. Hydrocarbons	0.4459	0.6557	0.7343	0.08
Ketones vs. Aldehydes	0.8242	0.4098	0.5737	0.27
Aldehydes vs. Acids	0.0000	1.000	1.000	0.00
Esters vs. Alcohols	−0.1021	0.9187	0.9527	0.02
Lactones vs. Ketones	−0.2430	0.8080	0.8701	0.06
Phenols vs. Esters	−0.5665	0.5711	0.6663	0.08
Ketones vs. Hydrocarbons	−1.134	0.2568	0.3994	0.29
Hydrocarbons vs. Esters	−0.7398	0.4594	0.5847	0.13
Lactones vs. Hydrocarbons	−1.190	0.2342	0.3857	0.26
Hydrocarbons vs. Alcohols	−1.245	0.2133	0.3857	0.25
Phenols vs. Alcohols	−1.085	0.2780	0.4097	0.17
Ketones vs. Esters	−1.261	0.2073	0.3857	0.23
Ketones vs. Alcohols	−1.834	0.0667 **	0.1868	0.40
Aldehydes vs. Alcohols	−1.875	0.0607 **	0.1868	0.44
Lactones vs. Esters	−1.868	0.0617 **	0.1868	0.31
Lactones vs. Alcohols	−2.289	0.0221 *	0.1547	0.44

* Significant at $\alpha = 0.05$. ** Marginal significant at $\alpha = 0.1$.

Although these findings no longer meet the conventional threshold for statistical significance, the effect size values (r) (Table 1) from each pairwise comparison suggest that the lack of strict statistical significance does not necessarily imply the absence of practical importance. For example, there are notable differences ($r \geq 0.5$) between phenols and acids, alcohols and acids, and hydrocarbons and acids. Additionally, there are medium to large differences ($0.3 < r < 0.5$) between esters and acids, hydrocarbons and aldehydes, ketones and alcohols, aldehydes and alcohols, and lactones and alcohols. These substantial effect size imply that, while the results may not be statistically significant according to traditional criteria, there may still be meaningful differences between these groups in terms of how much their detections are suppressed in vapor matrices with high ethanol concentration.

Given that this is an exploratory experiment, these results are valuable for offering meaningful insights and contributing to the broader understanding of how detection of an odorant can be suppressed by the presence of ethanol in the vapor matrix. Furthermore, this finding suggests that this effect may vary across different chemical groups, highlighting potential differences in the extent to which ethanol suppresses detection. These insights provide a foundation for future research, which can further explore with larger sample size and panel size.

3.2. Comparison of Degree of ODT Change (R) for the Same Odorants in the Presence or Absence of Ethanol/Water Liquid Matrices (Experiment 2)

Tables S2 and S3 list the ODTs of all four panelists for the seven tested odorants in the vapor matrices of 0% $ABV_{d.equiv.}$, 20% $ABV_{d.equiv.}$, or 40% $ABV_{d.equiv.}$, and in the liquid matrices of 0%, 20% and 40% ABV ethanol/water solutions. The Wilcoxon test was used to compare degree of ODT change between the presence and absence of liquid matrices

(Table 2). With liquid matrix, R is the ratio of individual ODT determined in the 20% ABV or 40% ABV ethanol/water solution, versus that determined in water (0% ABV ethanol/water solution) (denoted as $R_{20\%ABV}$ and $R_{40\%ABV}$, respectively). The sign of the Z-score (positive or negative) indicates the direction of the difference between the two groups. With the presence of a 20% ABV ethanol/water liquid matrix, the $R_{20\%ABV}$ value for most odorants tended to be higher than compared to the absence of the liquid matrix ($R_{20\%ABV\ d.equiv.}$), with the exception of γ-nonalactone. However, this difference was significant only for guaiacol, with β-damascenone showing marginal significance. When the liquid matrix was increased to 40% ABV, the direction of the differences remained the same, but the differences became significant for odorants such as ethyl butyrate, β-damascenone, and γ-nonalactone, while isoeugenol became marginally significant. Notably, the difference for guaiacol was no longer significant under this condition.

Table 2. Wilcoxon test comparison of log scaled ODT change (R) between presence ($R_{20\%ABV}$ and $R_{40\%ABV}$) and absence ($R_{20\%ABV\ d.equiv.}$ and $R_{40\%ABV\ d.equiv.}$) of liquid matrix, and between 20% ABV and 40% ABV liquid matrices.

Odorant	$R_{20\%ABV}$ vs. $R_{20\%ABV\ d.equiv.}$		$R_{40\%ABV}$ vs. $R_{40\%ABV\ d.equiv.}$	
	Z Score	*p*-Value	Z Score	*p*-Value
Ethyl isobutyrate	−1.607	0.1081	0.1461	0.8839
Ethyl butyrate	−1.340	0.1804	−2.191	0.0284 *
β-Damascenone	−1.935	0.0530 **	−2.233	0.0256 *
γ-Nonalactone	0.1461	0.8839	−2.372	0.0177 *
Guaiacol	−2.205	0.0275 *	−0.7304	0.4651
4-Ethyl guaiacol	−1.617	0.1059	−0.4465	0.6552
Isoeugenol (*E*)	−1.035	0.3005	−1.648	0.0994 **

* Significant at α = 0.05. ** Marginal significant at α = 0.1.

3.3. Gas/Liquid Coefficient (k_i) of Odorants in Water, 20%, and 40% ABV Ethanol/Water Solutions (Experiment 3)

Using the phase ratio variation method [24], the k_i values of seven selected odorants were determined in water, 20%, and 40% ABV ethanol/water solutions, with the results shown in Table 3. The k_i of ethyl butyrate (0.0150 ± 0.0071) and β-damascenone (0.0064 ± 0.0035) in water at 30 °C were in agreement with literature values. Tsachaki et al. [28] reported a k_i of 0.0163 for ethyl butyrate based on Henry's law constants from the EPI Suite™ v4.11 software, while Roberts et al. [29] reported a k_i of 0.0037 ± 0.0019 for β-damascenone.

Table 3. Gas/liquid coefficient (k_i) values for selected odorants in water, 20% ABV, and 40% ABV ethanol/water solutions.

Odorant	log P	B.P. (760 mmHg, °C)	k_i (Water)	k_i (20% ABV)	k_i (40% ABV)
Ethyl isobutyrate	1.648	112	0.0540 (0.0190) [a]	0.0150 (0.0071)	0.0144 (0.0033)
Ethyl butyrate	1.804	120	0.0150 (0.0071)	0.0080 (0.0028)	0.0075 (0.0035)
β-Damascenone	4.402	274	0.0064 (0.0035)		
			0.020 (0.014) [b]	0.0086 (0.0020) [b]	0.0053 (0.0019) [b]
γ-Nonalactone	1.942	243	0.00475 (0.00035) [b]	0.0225 (0.0035) [b]	0.0275 (0.0035) [b]
Guaiacol	1.320	205	0.0225 (0.0035)	0.0192 (0.0083)	0.0150 (0.0071)
4-Ethyl guaiacol	2.434	235	0.0120 (0.0028)	0.0134 (0.0047)	0.0150 (0.0024)
Isoeugenol (*E*)	3.040	266	0.0225 (0.0035)		
			0.030 (0.014) [b]	0.0196 (0.0041) [b]	0.013 (0.012) [b]

[a] Numbers in parenthesis represents standard deviations of two replications. [b] Partition coefficient was determined at 60 °C.

For β-damascenone, γ-nonalactone, and isoeugenol, their k_i values in the 20% and 40% ABV ethanol/water solutions could not be determined at 30 °C using the same

method. These odorants generally exhibit low volatility, and in ethanol/water solutions, the differences in peak areas resulting from changes in the phase ratio (β) were too slight to be reliably measured. This represented a limitation of this method. To address this, the temperature was increased to 60 °C with the intention to increase their volatility, allowing the phase ratio variation method to be applied and their k_i values in these two ethanol/water solutions to be determined. It was assumed that the trends observed in the k_i variation between the two solutions at 60 °C would be similar to those at 30 °C.

The results indicate that certain odorants, including ethyl isobutyrate, ethyl butyrate, β-damascenone, guaiacol, and isoeugenol, exhibit high volatility in water. However, their volatility decreases to varying extents as the ethanol concentration in the solution increases to 20%. For instance, k_i of ethyl isobutyrate decreases by a factor of 3.6, while that of β-damascenone drops by 2.3-fold. Ethyl butyrate experiences a reduction of approximately 1.9-fold, and isoeugenol shows a decrease of 1.5-fold. As the ethanol concentration rises to 40%, the k_i values continue to decline. β-Damascenone experiences an additional reduction of about 1.6-fold, and isoeugenol sees a consistent decrease by a factor of 1.5. In contrast, the k_i of ethyl isobutyrate and ethyl butyrate shows only slight decreases, with reductions of 4% and 6%, respectively. Notably, the k_i variation for guaiacol between water and ethanol/water solutions is relatively minor, exhibiting an overall decrease of 33% as the ethanol concentration increases to 40%.

On the other hand, γ-nonalactone and 4-ethyl guaiacol display different trends in their k_i variation. γ-Nonalactone exhibits low volatility in water, but this changes as the ethanol concentration increases. Specifically, its volatility increases by approximately 4.7-fold at 20% ABV, followed by an additional 1.2-fold increase when the ethanol concentration reaches 40%. 4-Ethyl guaiacol, however, exhibits a more consistent yet modest patten, with about a 12% increase in volatility at 20% ABV, followed by another 12% increase as the concentration rises to 40% ABV.

4. Discussion

The primary objective of this study was to demonstrate the isolated pharmacodynamic effect of ethanol on the ODTs of key odorants in distilled spirits models. To achieve this, we designed and conducted an experiment to determine the ODTs of thirty-four selected odorants in the absence of ethanol/water liquid matrices. By varying ethanol concentration in the vapor matrix, we observed a trend where the ODT of all tested odorants increased with rising ethanol concentration. This indicates that the presence of ethanol in the vapor matrix suppresses the detection of these odorants. However, the extent of this suppression is not uniform across all odorants; certain chemical groups, including alcohols, esters, hydrocarbons, and phenols, exhibit a more profound effect than others.

The published literature on the mechanism of olfactory sensation provides some potential explanation. The sense of smell starts at ORCs that are located in the olfactory epithelium (OE) within the nasal cavity. All components necessary for olfactory signal transduction are enriched in the olfactory cilia, which protrude into the mucus covering the surface of the OE [30]. The olfactory cilia are equipped with receptor proteins and enzymes that convert the chemical energy of odorants to electrical signals. There are four key steps in the detection and identification of an odorant [30,31], and any interruption in these steps can compromise the ability to detect it: first, odorants from the vapor phase must dissolve into the aqueous mucus, where they bind to odorant-binding proteins (OBPs) [32]. These OBPs enhance the activity of odorants and transport them across the nasal mucus to the receptor proteins located on the cilia bilayer membranes [32,33]; second, odorants must be recognized by the receptor proteins; third, the activated receptor proteins stimulate a G protein-coupled receptor (GPCRs) mechanism, which activates type III adenylyl cyclase. This enzyme converts ATP to cyclic AMP, which then binds and activates olfactory cyclic nucleotide-gated (CNG) channels; lastly, the opening of the CNG channels allows an inward flow of Ca^{2+} ions, which further activates Ca^{2+}-activated Cl^{-} channels, inducing an excitatory response.

The ODT of ethanol in air is 80 ppm (0.15 mg/L) [34]. It is speculated that at concentration higher than its ODT—such as 9.9 ± 1.3 mg/L at 20% $ABV_{d.equiv.}$ and 17.01 ± 0.61 mg/L at 40% $ABV_{d.equiv.}$ in this study—ethanol not only is perceived as an odorant, but also acts as an active agent, inducing a pharmacodynamic effect at the sites of ORCs. Specifically, the general suppression of odorant detection can be attributed to ethanol's impact on the lipid bilayer properties, which in turn leads to the suppression of CNG channels. Alcohols, including ethanol, are known to modulate the properties of lipid bilayer, affecting membrane protein functions [15,35]. Ethanol interacts with the phospholipid bilayer at the lipid-water interface, altering the orientation of the lipid headgroups and disrupting the lipid packing in the rigid region of the glycerol backbone [14]. This disordering affects the entire length of the acyl chains. Since CNG channels are densely expressed on the ciliary membrane [30], ethanol's disruption of the lipid bilayer likely suppresses many CNG channels simultaneously, inhibiting the inward flow of Ca^{2+} ions and thereby impeding olfactory signal transduction across all odorants. This disruption is likely concentration-depend, which would explain the observed increase in odorant suppression as ethanol concentration rises.

The varying degrees of detection suppression across chemical groups can be at least partially explained by competitive binding affinity to OBPs. OBPs are low molecular weight soluble proteins secreted by glands in the nasal cavity and released into the nasal mucus. They are responsible for transporting odorants across the aqueous nasal mucus to the olfactory receptor proteins [32,33]. The first ethanol-sensitive OBP, LUSH, was identified in the olfactory system of *Drosophila melanogaster* [36]. The crystal structure of the LUSH-ethanol complex revealed a specific binding pocket for ethanol [36,37]. Although no studies have yet identified this OBP in humans, it is likely that such a protein exists, possibly with a similar binding pocket that recognizes and transports ethanol. When other odorants have a similar molecular size or functional groups that form hydrogen bonds or hydrophobic interactions within the OBP pocket, a competitive binding between ethanol and these odorants likely occur. In the case, ethanol would have an advantage due to its higher abundance. For instance, in this study, one of the strongest detection suppressions was observed for 3-methyl-1-butanol, which could be attributed to the competitive binding with OBPs. This can be explained by the structural similarity between 3-methyl-1-butanol and n-butanol, the latter of which has been previously reported to bind to the ethanol-binding pocket in LUSH [37].

Olfactory receptor antagonism between ethanol and odorants is another potential explanation for the varying degrees of detection suppression observed across chemical groups. The detection of volatile odorants, including ethanol, is mediated by several hundred different GPCRs, with each odorant's identity encoded through a combinatorial receptor coding schema [38,39]. Different odorants are recognized by different, though sometimes overlapping, subsets of receptor proteins. As a results, in odorant mixtures, antagonism often occurs between components, where odorants can act as an both agonist and antagonist to olfactory receptors (ORs) [40]. In this study, ethanol may have acted as both an agonist for its own ORs and as an antagonist for the ORs responding to other odorants, likely due to its high abundance.

The pharmacodynamic effect of ethanol on ORCs may be even more complex. Previous studies have suggested that ethanol can directly interact with membrane proteins [41], and its impact on the lipid bilayer can also lead to activation of GPCRs [35], as well as the displacement of membrane-bound Ca^{2+} ions, which interferes with inward membrane current [17]. All of these factors could directly or indirectly affect olfactory signal transduction, providing a potential underlying mechanism for the results observed in the first study.

The second objective of this study was to determine the dominant ethanol-related factors—physicochemical versus pharmacodynamic—that influence the ODT of odorants in ethanol/water solutions. To achieve this, we conducted two complementary experiments; the first measured the ODTs of seven odorants in the presence of ethanol/water liquid matrices, and the second assessed the air/liquid partition coefficient (k_i) of these seven odorants in water, as well as in 20%, and 40% ABV ethanol/water solutions. By varying ethanol concentration in

the liquid matrix, we observed a consistent trend: the ODT of all tested odorants increased as ethanol concentration rose in the liquid matrices. However, unexpectedly, when comparing to the degree of ODT change (R) between the vapor matrix at 20% $ABV_{d.equi.}$ and the 20% ABV liquid matrix, as well as between the vapor matrix at 40% $ABV_{d.equi.}$ and the 40% ABV liquid matrix, the differences were not significant for most odorants, except β-damacenone. Odorants such as ethyl butyrate, γ-nonalactone, guaiacol, and isoeugenol only showed significance or marginal significance in one of the comparison pairs. This result was unexpected. It was anticipated that the ethanol/water liquid matrices would have a notable physicochemical effect on odorant solubility, altering the partition coefficient of odorants between the liquid and vapor phases. This, in turn, would affect the concentration of odorants in the vapor matrix, thereby enhancing or reducing odorant detection due to changes in odorant concentration. While ethanol's pharmacodynamic effect already suppressing odorant detection, an increase or decrease in odorant concentration in the vapor matrix should have significantly amplified or diminished their detection, resulting in more noticeable differences in the degree of ODT change (R). Additionally, after analyzing how the k_i values changed with increasing ethanol concentration, we found that the variations in k_i for each odorant across different ethanol/water solutions does not agree with their degree of ODT changes. The differences between k_i values were not as significant as anticipated. The changes were slightly more pronounced between water and 20% ABV, but there was little difference between 20% and 40% ABV. For example, the k_i values for ethyl isobutyrate and ethyl butyrate only decreased 4% and 6%, respectively. This led us to interpretate that from water to 20% ABV ethanol/water solution, the physicochemical effect did influence the solubility of odorants, impacting their detection to some extent. However, as ethanol concentration increased from 20% to 40%, the physicochemical effect became less pronounced, having minimal impact on the volatility of odorants. It's important to note that as ethanol concentration increased in the liquid matrix, it also rose in the vapor matrix, thereby enhancing its pharmacodynamic effect and further suppressing odorant detection. Based on the k_i measurements and the observed changes with ethanol concentration, it is likely that the observed results are primarily due to the increased ethanol concentration in the vapor matrix, which intensified the pharmacodynamic effect. The changes in the partition coefficients likely contributed only slightly, reflecting a limited physicochemical impact.

5. Conclusions

When the ethanol concentration in the spirit's liquid matrix changes, it not only influences the concentration of odorants in the headspace but also alters the ethanol concentration in the vapor matrix itself. Our three experiments collectively demonstrated that the pharmacodynamic effect of ethanol, driven by its concentration in the vapor matrix, is the primary factor affecting odorant detection. These findings support the practice of diluting ethanol content in distilled spirits by half (from 40% to 20% ABV) or using differently shaped glass vessels during nosing, as both methods reduce ethanol concentration in the vapor matrix, thereby diminishing its pharmacodynamic effect at the ORCs and allowing other odorants to be more easily detected.

In these exploratory studies, only one odorant was evaluated at a time in either the vapor matrices or the liquid matrices. However, when two or more odorants are present in these matrices, the situation becomes more complex. In addition to ethanol effects we discussed, interactions between odorants in the liquid matrix and in the nasal cavity may also occur, which can further influence ODT of odorants. While it would be interesting to investigate these interactions in future studies, they were beyond the scope of this work.

Supplementary Materials: The following supporting information can be downloaded at: https://www.mdpi.com/article/10.3390/beverages10040116/s1, Table S1: individual (panel 1) ODT (μg) of odorants in the 0% $ABV_{d.equiv.}$, 20% $ABV_{d.equiv.}$ and 40% $ABV_{d.equiv.}$ vapor matrices; Table S2: individual (panel 2) ODT (μg) of odorants in the 0% $ABV_{d.equiv.}$, 20% $ABV_{d.equiv.}$ and 40% $ABV_{d.equiv.}$ vapor matrices; Table S3; individual (panel 2) ODT (ppd) of odorants in the 0% ABV, 20% ABV, and 40% ABV ethanol/water solutions.

Author Contributions: Conceptualization, Z.W. and K.R.C.; methodology, Z.W. and K.R.C.; software, Z.W.; validation, Z.W. and K.R.C.; formal analysis, Z.W.; investigation, Z.W. and K.R.C.; resources, Z.W.; data curation, Z.W.; writing—original draft preparation, Z.W.; writing—review and editing, K.R.C.; supervision, K.R.C.; project administration, K.R.C.; funding acquisition, K.R.C. All authors have read and agreed to the published version of the manuscript.

Funding: Funding of this project was provided by the National Institute of Food and Agricultura, U.S. Department of Agriculture, under Project ILLU-698-987.

Data Availability Statement: The data underlying this article are available in the article and in its online Supplemental Materials.

Conflicts of Interest: For commercial affiliations, all authors must be accounted for. We recommend using Author Zhuzhu Wang was employed by the University of Illinois during the study design, the following template: execution, data collection, analysis, interpretation, and writing of this article. After graduation, author Zhuzhu Wang began working for the Archer Daniels Midland Company (ADM). The company (ADM) was not involved in the study design, execution, data collection, analysis, interpretation, and writing of this article or the decision to submit it for publication. The authors declare that the research was conducted in the absence of any commercial or financial relationships that could be construed as a potential conflict of interest.

References

1. Genthner-Kreger, E.; Cadwallader, K.R. Identification of rotundone as an important contributor to the flavor of oak-aged spirits. *Molecules* **2021**, *26*, 4368. [CrossRef]
2. Glabasnia, A.; Hofmann, T. Sensory-directed identification of taste-active ellagitannins in american (quercus alba l.) and european oak wood (quercus robur l.) and quantitative analysis in bourbon whiskey and oak-matured red wines. *J. Agric. Food Chem.* **2006**, *54*, 3380–3390. [CrossRef]
3. Zhu, W.; Cadwallader, K.R. Streamlined approach for careful and exhaustive aroma characterization of aged distilled liquors. *Food Chem. X* **2019**, *3*, 100038–100047. [CrossRef] [PubMed]
4. Winstel, D.; Gammacurta, M.; Waffo-Téguo, P.; Marchal, A. Identification of two new taste-active compounds in oak wood: Structural elucidation of potential β-methyl-γ-octalactone precursors and quantification in spirits. *J. Agric. Food Chem.* **2024**, *72*, 20592–20602. [CrossRef]
5. Ickes, C.M.; Cadwallader, K.R. Effects of ethanol on flavor perception in alcoholic beverages. *Chemosens. Percept.* **2017**, *10*, 119–134. [CrossRef]
6. Wang, Z.; Ickes, C.M.; Cadwallader, K.R. Influence of ethanol on flavor perception in distilled spirits. In *Sex, Smoke, and Spirits: The Role of Chemistry*; American Chemical Society: Washington, DC, USA, 2019; pp. 277–290.
7. Ickes, C.M.; Cadwallader, K.R. Effect of ethanol on flavor perception of rum. *Food Sci. Nutr.* **2018**, *6*, 912–924. [CrossRef] [PubMed]
8. Harwood, W.S.; Parker, M.N.; Drake, M. Influence of ethanol concentration on sensory perception of rums using temporal check-all-that-apply. *J. Sens. Stud.* **2020**, *35*, e12546. [CrossRef]
9. Shuttleworth, E.E.; Apóstolo, R.F.; Camp, P.J.; Conner, J.M.; Harrison, B.; Jack, F.; Clark-Nicolas, J. Molecular dynamics simulations of flavour molecules in scotch whisky. *J. Mol. Liq.* **2023**, *383*, 122152. [CrossRef]
10. Patel, S.J.; Bollhoefer, A.D.; Doty, R.L. Influences of ethanol ingestion on olfactory function in humans. *Psychopharmacology* **2004**, *171*, 429–434. [CrossRef]
11. Rupp, C.I.; Kurz, M.; Kemmler, G.; Mair, D.; Hausmann, A.; Hinterhuber, H.; Fleischhacker, W.W. Reduced olfactory sensitivity, discrimination, and identification in patients with alcohol dependence. *Alcohol. Clin. Exp. Res.* **2003**, *27*, 432–439. [CrossRef]
12. Austin, S.; Scholfield, C. Interaction between phorbol dibutyrate and anaesthetics on synaptic responses from olfactory cortex of rat. *Neuropharmacology* **1991**, *30*, 1113–1118. [CrossRef] [PubMed]
13. Nicoll, R.A. The effects of anaesthetics on synaptic excitation and inhibition in the olfactory bulb. *J. Physiol.* **1972**, *223*, 803–814. [CrossRef] [PubMed]
14. Barry, J.A.; Gawrisch, K. Direct nmr evidence for ethanol binding to the lipid-water interface of phospholipid bilayers. *Biochemistry* **1994**, *33*, 8082–8088. [CrossRef] [PubMed]
15. Ingólfsson, H.I.; Andersen, O.S. Alcohol's effects on lipid bilayer properties. *Biophys. J.* **2011**, *101*, 847–855. [CrossRef]
16. Patra, M.; Salonen, E.; Terama, E.; Vattulainen, I.; Faller, R.; Lee, B.W.; Holopainen, J.; Karttunen, M. Under the influence of alcohol: The effect of ethanol and methanol on lipid bilayers. *Biophys. J.* **2006**, *90*, 1121–1135. [CrossRef]
17. Seeman, P. The membrane actions of anesthetics and tranquilizers. *Pharmacol. Rev.* **1972**, *24*, 583–655.
18. Takeuchi, H.; Ishida, H.; Hikichi, S.; Kurahashi, T. Mechanism of olfactory masking in the sensory cilia. *J. Gen. Physiol.* **2009**, *133*, 583. [CrossRef] [PubMed]
19. Ingólfsson, H.I.; Andersen, O.S. Screening for small molecules' bilayer-modifying potential using a gramicidin-based fluorescence assay. *Assay Drug Dev. Technol.* **2010**, *8*, 427–436. [CrossRef]

20. Williams, R.C.; Sartre, E.; Parisot, F.; Kurtz, A.J.; Acree, T.E. A gas chromatograph-pedestal olfactometer (gc-po) for the study of odor mixtures. *Chemosens. Percept.* **2009**, *2*, 173–179. [CrossRef]
21. Dunkel, A.; Steinhaus, M.; Kotthoff, M.; Nowak, B.; Krautwurst, D.; Schieberle, P.; Hofmann, T. Nature's chemical signatures in human olfaction: A foodborne perspective for future biotechnology. *Angew. Chem. Int. Ed. Engl.* **2014**, *53*, 7124–7143. [CrossRef]
22. *ASTM E679-19*; Standard Practice for Determination of Odor and Taste Thresholds by a Forced-Choice Ascending Concentration Series Method of Limits. ASTM International: West Conshohocken, PA, USA, 2019.
23. Buttery, R.G.; Seifert, R.M.; Guadagni, D.G.; Ling, L.C. Characterization of additional volatile components of tomato. *J. Agric. Food Chem.* **1971**, *19*, 524–529. [CrossRef]
24. Ettre, L.; Welter, C.; Kolb, B. Determination of gas-liquid partition coefficients by automatic equilibrium headspace-gas chromatography utilizing the phase ratio variation method. *Chromatographia* **1993**, *35*, 73–84. [CrossRef]
25. Hedner, M.; Larsson, M.; Arnold, N.; Zucco, G.M.; Hummel, T. Cognitive factors in odor detection, odor discrimination, and odor identification tasks. *J. Clin. Exp. Neuropsychol.* **2010**, *32*, 1062–1067. [CrossRef] [PubMed]
26. Larsson, M.; Finkel, D.; Pedersen, N.L. Odor identification: Influences of age, gender, cognition, and personality. *J. Gerontol. B Psychol. Sci. Soc. Sci.* **2000**, *55*, P304–P310. [CrossRef] [PubMed]
27. Laing, D.G.; Panhuber, H.; Slotnick, B. Odor masking in the rat. *Physiol. Behav.* **1989**, *45*, 689–694. [CrossRef]
28. Tsachaki, M.; Linforth, R.S.; Taylor, A.J. Dynamic headspace analysis of the release of volatile organic compounds from ethanolic systems by direct apci-ms. *J. Agric. Food Chem.* **2005**, *53*, 8328–8333. [CrossRef]
29. Roberts, D.D.; Pollien, P.; Antille, N.; Lindinger, C.; Yeretzian, C. Comparison of nosespace, headspace, and sensory intensity ratings for the evaluation of flavor absorption by fat. *J. Agric. Food Chem.* **2003**, *51*, 3636–3642. [CrossRef]
30. Takeuchi, H.; Kurahashi, T. Olfactory transduction channels and their modulation by varieties of volatile substances. In *Taste and Smell*; Springer: Cham, Switzerland, 2017; pp. 115–149.
31. Kurahashi, T.; Lowe, G.; Gold, G.H. Suppression of odorant responses by odorants in olfactory receptor cells. *Science* **1994**, *265*, 118–120. [CrossRef] [PubMed]
32. Archunan, G. Odorant binding proteins: A key player in the sense of smell. *Bioinformation* **2018**, *14*, 36. [CrossRef]
33. Gonçalves, F.; Ribeiro, A.; Silva, C.; Cavaco-Paulo, A. Biotechnological applications of mammalian odorant-binding proteins. *Crit. Rev. Biotechnol.* **2021**, *41*, 441–455. [CrossRef]
34. Amoore, J.E.; Hautala, E. Odor as an ald to chemical safety: Odor thresholds compared with threshold limit values and volatilities for 214 industrial chemicals in air and water dilution. *J. Appl. Toxicol.* **1983**, *3*, 272–290. [CrossRef] [PubMed]
35. Mitchell, D.C.; Lawrence, J.T.; Litman, B.J. Primary alcohols modulate the activation of the g protein-coupled receptor rhodopsin by a lipid-mediated mechanism. *J. Biol. Chem.* **1996**, *271*, 19033–19036. [CrossRef] [PubMed]
36. Kruse, S.W.; Zhao, R.; Smith, D.P.; Jones, D.N.M. Structure of a specific alcohol-binding site defined by the odorant binding protein lush from drosophila melanogaster. *Nat. Struct. Mol. Biol.* **2003**, *10*, 694–700. [CrossRef] [PubMed]
37. Bucci, B.K.; Kruse, S.W.; Thode, A.B.; Alvarado, S.M.; Jones, D.N. Effect of n-alcohols on the structure and stability of the drosophila odorant binding protein lush. *Biochemistry* **2006**, *45*, 1693–1701. [CrossRef]
38. Kajiya, K.; Inaki, K.; Tanaka, M.; Haga, T.; Kataoka, H.; Touhara, K. Molecular bases of odor discrimination: Reconstitution of olfactory receptors that recognize overlapping sets of odorants. *J. Neurosci.* **2001**, *21*, 6018–6025. [CrossRef]
39. Malnic, B.; Hirono, J.; Sato, T.; Buck, L.B. Combinatorial receptor codes for odors. *Cell* **1999**, *96*, 713–723. [CrossRef]
40. Oka, Y.; Omura, M.; Kataoka, H.; Touhara, K. Olfactory receptor antagonism between odorants. *EMBO J.* **2004**, *23*, 120–126. [CrossRef]
41. Aryal, P.; Dvir, H.; Choe, S.; A Slesinger, P. A discrete alcohol pocket involved in girk channel activation. *Nat. Neurosci.* **2009**, *12*, 988–995. [CrossRef]